Nephron

Clinical Practice: Research Article

Nephron
DOI: 10.1159/000534893

Received: August 2, 2023
Accepted: October 25, 2023
Published online: November ▪▪▪, 2023

# Functional Magnetic Resonance Imaging to Monitor Disease Progression: A Prospective Study in Patients with Primary Membranoproliferative Glomerulonephritis

Giulia Villa[a] Erica Daina[a] Paolo Brambilla[b] Sara Gamba[a] Valentina Fanny Leone[a] Camillo Carrara[c] Paola Rizzo[a] Marina Noris[a] Giuseppe Remuzzi[a] Andrea Remuzzi[d] Anna Caroli[a]

[a]Istituto di Ricerche Farmacologiche Mario Negri IRCCS, Bergamo, Italy; [b]Unit of Radiology, ASST Papa Giovanni XXIII, Bergamo, Italy; [c]Unit of Nephrology and Dialysis, ASST Papa Giovanni XXIII, Bergamo, Italy; [d]Department of Management, Information and Production Engineering, University of Bergamo, Bergamo, Italy



**Keywords**
Magnetic resonance imaging · Kidney · Membranoproliferative glomerulonephritis · Rare diseases · Disease progression

**Abstract**

***Introduction:*** Primary membranoproliferative glomerulonephritis (MPGN) is a rare kidney disease with poor prognosis and no specific therapies. The disease heterogeneity and the difficulty of performing repeated kidney biopsies pose big challenges. This study investigates the correlation between non-contrast enhanced magnetic resonance imaging (MRI) and histologic and clinical findings in patients with primary MPGN. ***Methods:*** Patients with primary MPGN underwent baseline and 1-year kidney MRI in addition to biopsy and laboratory testing as part of a prospective MRI subproject of a clinical trial (ClinicalTrials.gov identifier NCT03723512). Diffusion-weighted and phase-contrast MRI were used to investigate kidney diffusivity and perfusion. Peritubular interstitial volume and fibrosis were quantified on kidney biopsies. ***Results:*** Seven patients with primary MPGN (18 [17–21] years, 43% females) were included. Kidney biopsies showed variable degree of global and segmental glomerular sclerosis ([5–30]% and [10–60]%), mild interstitial fibrosis (<10%), and increased peritubular interstitial volume ([19–40]%). MRI and laboratory parameters changed very differently from patient to patient over 1 year. Peritubular interstitial volume and glomerular sclerosis negatively associated with renal blood flow (RBF) (rho = −0.81 and −0.77), and positively with renal vascular resistance (RVR) (rho = 0.65 and 0.73). Urinary albumin to creatinine ratio (uACR) negatively associated with RBF and filtration fraction (FF) (rho = −0.86 and −0.6), while positively with RVR (rho = 0.88). uACR decrease was associated with kidney diffusivity increase (rho = −0.5). Measured glomerular filtration rate (GFR) positively associated with kidney diffusivity, RBF, and FF (rho = 0.87, 0.85, and 0.59), while negatively with RVR (rho = −0.89); GFR increase was associated with kidney diffusivity, RBF, and FF increase (rho = 0.77, 0.7, and 0.7) and RVR decrease (rho = −0.7). ***Conclusion:*** The strong correlation found between MRI and histologic and clinical findings, despite

karger@karger.com
www.karger.com/nef



Correspondence to:
Anna Caroli, anna.caroli@marionegri.it

the rather limited number of patients, highlights MRI potential to monitor disease progression in patients with rare kidney disease.


## Introduction

Membranoproliferative glomerulonephritis (MPGN) is a pattern of glomerular injury observed in kidney biopsies, with characteristic light microscopic changes: mesangial hypercellularity, endocapillary proliferation, and duplication – double contours – of the glomerular basement membrane [1]. In 2011, a classification on the basis of immunofluorescence was proposed [2, 3] that divides MPGN into different subtypes: (1) immune complex-associated MPGN (IC-MPGN), characterized by significant glomerular immunoglobulin (Ig) and complement deposition and (2) C3 glomerulopathy (C3G), with dominant glomerular C3 deposition (at least two orders of intensity stronger than any other immune reactant) and little or no Ig deposition. Using electron microscopy (EM), C3G may be further classified as: (1) dense deposit disease (DDD), with highly electron-dense deposits in the glomerular basement membrane; and (2) C3 glomerulonephritis, lacking the typical deposits of DDD [4].

MPGN may be primary or secondary to another disorder and an underlying cause is present in the majority of cases. When chronic infections, autoimmune diseases, or paraprotein-related kidney diseases are ruled out, and a clear underlying etiology cannot be identified, MPGN is considered primary or idiopathic.

Primary MPGN is a rare disease; patients cannot benefit from specific therapies, and their prognosis is poor with a high risk of end-stage renal disease within 5 to 10 years of diagnosis [5, 6]. After years of ineffective nonspecific treatments, several drugs that target at different levels the complement system, which is the core of disease pathogenesis, are currently under investigation for primary MPGN. However, clinical trials to test new therapeutics will be challenging and heavily influenced by the heterogeneity of the disease. Repeated kidney biopsies would be needed to accurately monitor disease progression and response to treatment over time. However, such biopsies may carry the risk of complications, are hard to accept by patients and susceptible to sampling bias, and thus difficult to perform repeatedly to assess serial changes.

Recent advances in functional and quantitative renal magnetic resonance imaging (MRI) research have made available techniques that can generate quantitative imaging biomarkers with the potential to improve the management of kidney diseases [7]. In particular, MRI techniques show great potential (1) to detect early signs of renal involvement, (2) to provide insight into the pathogenesis of underlying kidney disease, (3) to allow individual patient stratification in terms of prognosis, and (4) to monitor response to therapy. MRI biomarkers are unique among diagnostic tools in that they characterize the entire kidney in high-spatial detail, are able to detect cortico-medullary changes and left-right differences, and can assess the degree of functional heterogeneity within the kidney. In addition, MRI measures are well suited to repeated application since, at variance with other imaging techniques such as CT, do not need intravenous contrast agents and do not expose the patient to the risks of ionizing radiation [8]. Serial MRI studies have the potential to show structural and functional changes, providing valuable information on renal disease progression.

Among renal MRI techniques, renal diffusion-weighted MRI (DWI), providing detailed microstructural and functional information, has been increasingly used to localize the renal damage and assess its significance even before renal function declines, to predict renal function evolution and to follow microstructure changes occurring under treatment in chronic kidney diseases such as glomerulonephritis, diabetic nephropathy, hypertensive nephropathy, and kidney allograft dysfunction [9]. In addition, phase-contrast MRI (PC-MRI) allows to assess renal perfusion [10], providing complementary information. The present study examines the correlation between MRI parameters and histologic and clinical markers of disease course in patients with primary MPGN.

## Materials and Methods

*Patients*

All patients were enrolled in an MRI subproject of a phase II, single-arm, open-label, 12-month trial of patients with biopsy-confirmed primary MPGN treated with Danicopan, a small, orally active inhibitor of factor D that specifically inhibits the alternative pathway of complement system (ClinicalTrials.gov identifier NCT03723512). Key inclusion criteria were age between 17 and 65 years; diagnosis of primary MPGN confirmed by the central pathology; no more than 50% global fibrosis and no more than 50% of glomeruli with cellular crescents at pretreatment biopsy; clinical evidence of active disease based on significant proteinuria (defined as ≥500 mg/day of protein in a 24-h urine); stable dose of anti-proteinuric medications; enrolment in the ACH471-205 clinical study (ClinicalTrials.gov Identifier NCT03459443) at the Istituto di Ricerche Farmacologiche Mario Negri IRCCS, Ranica (BG), Italy; and no contraindications to perform MRI.

The study was reviewed and approved by the Local Ethics Committee (Comitato Etico della Provincia di Bergamo), approval number 179-18. Written informed consent was obtained from all adults or parents for minor patients. All patients underwent non-contrast enhanced (NCE)-MRI in addition to kidney biopsy, clinical evaluation, laboratory testing, and glomerular filtration rate (GFR) measurement at two time points (before and after 1 year of treatment with Danicopan, or at treatment discontinuation).

*NCE-MRI Acquisition*

MRI scans were acquired at the ASST Papa Giovanni XXIII (Bergamo, Italy) on a 1.5T clinical scanner (Optima MR450wGEM; General Electrics Healthcare), using a Phased Array 32-channel Torso Body Coil, with no contrast media injection. Structural MR sequences (T2 single shot fast spin-echo, FIESTA 3D spoiled gradient echo, and T1-3D spoiled gradient echo) were used to investigate renal anatomy. The following sequences were also acquired: (i) DWI, to provide information on water diffusion and fluid flowing in renal tissue; (ii) MR angiography, to depict the abdominal vessel structure; (iii) 2D PC-MRI, to assess renal artery blood flow. MRI sequences were acquired in a single acquisition session. Acquisition details are provided in online supplementary material (for all online suppl. material, see https://doi.org/10.1159/000534893).

*NCE-MRI Processing*

NCE-MRI processing was performed at the Medical Imaging Laboratory of the Istituto di Ricerche Farmacologiche Mario Negri IRCCS. Upon receipt, MR images underwent a careful quality control.

Total Kidney Volume

Each kidney was manually outlined on T1-weighted MRI scans using the polygon tool of ImageJ software [11] (NIH, Bethesda, MD, USA), by manually drawing a polyline on all contiguous slices. Single kidney volume was computed as the sum of the surface area of all the kidney outlines, multiplied by the slice thickness. Total kidney volume was computed as the sum of right and left volumes.

Diffusion-Weighted MRI

DWI scans were motion-corrected and DWI signal was interpreted using both a monoexponential model (allowing to compute the apparent diffusion coefficient, ADC) and a segmented fitted approach (allowing to compute pure diffusion – D, pseudo-diffusion – D*, and flowing fraction – F). Model fitting was performed by in-house software written in Matlab, after excluding any image showing artefact or inadequate quality. DWI parameter maps were averaged over whole kidney volume, cortex, and medulla. The difference between cortex and medullary values was computed for both ADC (Δ ADC) and D (ΔD). Additional details are available in online supplementary material.

Phase-Contrast MRI

For each PC-MRI scan, renal artery was outlined on the registered anatomical images. The renal artery average velocity profile was computed and blood flow was averaged over all phases. Total renal artery blood flow (RBF) was computed as sum of left and right renal artery flow. Renal plasma flow (RPF) was computed as RBF * (1 – hematocrit). Filtration fraction (FF) was computed as GFR/RPF*100. Finally, renal vascular resistance (RVR) was computed as mean arterial pressure divided by RPF. Additional details are available in online supplementary material.

*Histologic Characterization*

Qualitative Evaluation

Findings by light microscopy were jointly scored by two independent pathologists for severity on a semiquantitative scale (0–3+). Specifically, the scale was based on the proportion of glomeruli or percentage of cortical area displaying the described lesion, with 1–25% involvement described as 1+, 26–50% involvement as 2+, and more than 50% involvement as 3+. Selection of pathology parameters was based on previously published histologic index [12].

Light Microscopy

Routine processing pipelines were used for specimen preparation. Duboscq-Brasil-fixed, paraffin-embedded kidney tissue was cut at 3 μm thickness, deparaffinized and stained with periodic acid-Schiff (PAS) reagent. Biopsy specimens stained with PAS were imaged by a Zeiss Axio Imager.Z2 microscope with motorized stage using an EC Plan-Neofluar ×20 objective lens with 0.5 numerical aperture and Axiovision 4.8.2 acquisition software. To assess the collagen content, Duboscq-Brasil-fixed paraffin-embedded sections were stained with picric acid-Sirius red solution and analyzed using both standard light microscopy and polarized light resulting in birefringence of the collagen fibers.

Peritubular Interstitial Volume Quantification

Interstitial volume was quantified on biopsy specimens stained with PAS by point counting on each frame, using the ImageJ software. In details, a random offset grid (with 26 × 19 points, area per point = 10,000 pixels$^2$) was placed on each frame using the Grid plugin. Grid points falling in the peritubular interstitial space were counted on each frame separately using the cell counter plugin. The interstitial volume was finally computed as average ratio of number of grid points falling in the peritubular interstitial volume to number of points internal to the histologic sample.

Fibrosis Quantification

Fibrosis was quantified on biopsy specimens stained with Sirius Red and analyzed using polarized light, using the ImageJ software. First, individual frames were visually inspected: any nonrenal tissue (e.g., blank portion in case of partial coverage) and artifact were masked, and individual frames with <50% renal tissue coverage were excluded from quantification. Then each image was converted to gray scale and thresholded based on an image-specific cut-off defined as minimum value ensuring full background signal removal. Fibrosis percentage was finally computed as average ratio of fibrosis to renal tissue coverage areas.

*Laboratory Assessments*

Collected urine samples were assayed for total protein concentration, albumin and creatinine concentrations, urinary albumin to creatinine ratio (uACR), protein to creatinine ratio (uPCR), and total volume. Serum C3 concentrations were determined by immunoturbidimetric assay (Tina-quant) on a Cobas analyzer (Roche Diagnostics, Switzerland).

GFR was measured by the Iohexol plasma clearance technique [13], with blood samples collected at 120, 180, 240, 300, 360, 420,

**Table 1.** Sociodemographic features and histologic subclassification of the 7 patients with primary MPGN included in the study

| Patient | Gender | Age at onset | Age at study entry | Histologic subtype |
|---|---|---|---|---|
| #001 | M | 19 | 30 | C3GN |
| #002 | F | 11 | 18 | C3GN |
| #003 | M | 16 | 17 | DDD |
| #004 | F | 11 | 17 | C3GN |
| #005 | M | 10 | 18 | C3GN |
| #006 | F | 16 | 22 | C3GN |
| #007 | M | 17 | 20 | IC-MPGN |

C3GN, complement 3 glomerulonephritis; DDD, dense deposit disease; IC-MPGN, immune complex mediated membranoproliferative glomerulonephritis.

and 480 min after iohexol injection. In addition, GFR was estimated by the chronic kidney disease epidemiology collaboration (CKD-EPI) formula [14].

*Statistical Analysis*

Percent change between 1-year follow-up and baseline data was computed as (follow-up-baseline)/baseline data. The correlation between MRI parameters and histologic, clinical, and laboratory findings, as well as the correlation between changes in MRI parameters and in clinical and laboratory findings were investigated by Spearman's correlation. Significance threshold was set at $p < 0.05$. All statistical analyses were performed using R software (www.r-project.org), version 4.0.2.

## Results

Seven patients with primary MPGN were included in the study. Patients were aged 18 [15–19] years (median [IQR]) at study inclusion, and 43% of them were females (Table 1).

All patients underwent baseline kidney biopsy, and repeated NCE-MRI, laboratory testing, and GFR measurement at baseline and after 1-year follow-up. Follow-up kidney biopsy was performed in 2 patients.

*Kidney MRI, Laboratory, and Histologic Findings*

Kidney MRI parameters, computed at baseline and 1-year follow-up in individual patients, are summarized in Table 2, along with their percent change. MRI parameters changed very differently from patient to patient over 1 year. Some patients showed a clear improvement of the MRI picture (most noticeable in patient #003), with increased diffusivity in the whole kidney, cortex, and medulla, increased difference between cortical and medullary ADC (ΔADC), ΔD turning positive, increased RBF, RPF, and FF, and decreased RVR. Conversely, some patients showed a worsening of the MRI picture (patients #001, #004, and #005), with decreased diffusivity, RBF, RPF, and FF, and increased RVR. In other patients (for instance #002), the MRI picture did not significantly change.

Laboratory findings in individual patients at baseline and 1-year follow-up are reported in Table 3, along with their percent change. uPCR and uACR on urine spot significantly decreased relative to baseline in 2 patients (#002 and #003) together with the increase of serum C3 concentration and improvement in renal function parameters (serum creatinine, eGFR, measured GFR [mGFR]). A variable progression of kidney disease despite treatment was observed in the other 5 patients.

Histologic findings for all patients at baseline kidney biopsy are summarized in Table 4. All kidney biopsies at baseline showed a membranoproliferative pattern of injury (histologic subclassification was C3 glomerulonephritis in 5 patients, DDD in 1 patient, and IC-MPGN in 1 patient). The degree of global and segmental glomerular sclerosis was quite variable and ranged from 5 to 30% and from 10 to 60%, respectively. Every case displayed at least moderate glomerular inflammation, represented by mesangial proliferation and leukocyte infiltration. Crescents were detected only in the biopsy from patient #003. While overall interstitial fibrosis was mild (<10%), peritubular interstitial volume was significantly increased and ranged from 18.6% to 40.3%.

*Correlation between MRI and Histologic Findings*

Peritubular interstitial volume, assessed at all available time points, was negatively associated with RBF and RPF (rho = −0.81, $p = 0.022$ and rho = −0.52, $p = 0.200$, respectively) and positively associated with RVR (rho = 0.65, $p = 0.083$) (Fig. 1a). No significant correlation was found between any MRI parameter and interstitial fibrosis (Fig. 1b). Both global and segmental glomerular sclerosis were negatively associated with RBF and RPF (global: rho = −0.77, $p = 0.021$ and rho = −0.73, $p = 0.031$; segmental: rho = −0.58, $p = 0.100$ and rho = −0.47, $p = 0.200$, respectively) and positively associated with RVR (global: rho = 0.73, $p = 0.026$; segmental: 0.67, $p = 0.047$) (Fig. 1c, d).

*Correlation between MRI and Laboratory Findings*

At baseline all patients had extremely low serum C3 values (less than 25, with [90–180] normal range) due to the disease-induced C3 extra-consumption, and it was not possible to establish a correlation between C3 and MRI parameters. Although C3 levels remained lower than normal for all patients, after 1-year follow-up 3 patients showed an increase (Δ ≥100%). In these patients, higher C3 was associated with higher diffusivity, higher RBF, higher FF, and lower RVR (Fig. 2).

**Table 2.** Kidney MRI results at baseline and 1-year follow-up in the 7 patients with primary MPGN included in the study

| | D kidney, $10^{-3}$ mm$^2$/s | D cortex, $10^{-3}$ mm$^2$/s | D medulla, $10^{-3}$ mm$^2$/s | ΔD, $10^{-3}$ mm$^2$/s | ADC kidney, $10^{-3}$ mm$^2$/s | ADC cortex, $10^{-3}$ mm$^2$/s | ADC medulla, $10^{-3}$ mm$^2$/s | ΔADC, $10^{-3}$ mm$^2$/s | RBF, mL/min | RPF, mL/min | FF, % | RVR (dyn*s/cm$^5$) | TKV, mL |
|---|---|---|---|---|---|---|---|---|---|---|---|---|---|
| #001 | | | | | | | | | | | | | |
| Baseline | 1.77 (1.52–1.98) | 1.77 (1.54–1.98) | 1.75 (1.51–1.94) | 0.018 | 2.50 (2.14–3.01) | 2.27 (1.94–2.65) | 2.42 (2.10–2.78) | −0.146 | 1,039 | 730 | 4.94 | 0.12 | 671 |
| 1 year | 1.53 (1.30–1.75) | 1.44 (1.26–1.66) | 1.51 (1.32–1.69) | −0.076 | 2.26 (1.99–2.67) | 2.37 (2–04-2.70) | 2.55 (2.21–2.95) | −0.184 | 398 | 294 | 4.55 | 0.3 | 527 |
| Δ, % | −14 | −18 | −14 | | −9 | 4 | 6 | | −62 | −60 | −8 | 158 | −21 |
| #002 | | | | | | | | | | | | | |
| Baseline | 1.62 (1.46–1.78) | 1.57 (1.41–1.76) | 1.57 (1.44–1.70) | 0.017 | 2.77 (2.50–3.16) | 2.85 (2.57–3.21) | 2.60 (2.39–2.83) | 0.249 | 1,150 | 717 | 12.15 | 0.08 | 521 |
| 1 year | 1.62 (1.44–1.82) | 1.62 (1.44–1.83) | 1.61 (1.45–1.80) | 0.008 | 2.75 (2.43–3.12) | 2.91 (2.57–3.28) | 2.65 (2.42–2.87) | 0.253 | 1,204 | 725 | 16.52 | 0.07 | 494 |
| Δ, % | 0 | 3 | 3 | | −1 | 2 | 2 | | 5 | 1 | 36 | −14 | −5 |
| #003 | | | | | | | | | | | | | |
| Baseline | 1.54 (1.42–1.65) | 1.49 (1.38–1.59) | 1.54 (1.44–1.64) | −0.055 | 1.91 (1.74–2.14) | 1.91 (1.74–2.01) | 1.87 (1.73–2.02) | 0.042 | 1,076 | 768 | 6.09 | 0.09 | 460 |
| 1 year | 1.70 (1.53–1.87) | 1.75 (1.60–1.91) | 1.69 (1.54–1.85) | 0.059 | 2.55 (2.30–2.86) | 2.55 (2.30–2.86) | 2.45 (2.30–2.72) | 0.140 | NA | NA | NA | NA | 377 |
| Δ, % | 11 | 17 | 9 | | 34 | 38 | 34 | | NA | NA | NA | NA | −18 |
| #004 | | | | | | | | | | | | | |
| Baseline | 1.53 (1.42–1.68) | 1.57 (1.46–1.70) | 1.50 (1.41–1.60) | 0.066 | 2.13 (1.92–2.41) | 2.13 (1.92–2.35) | 2.06 (1.88–2.24) | 0.065 | 786 | 592 | 5.7 | 0.11 | 385 |
| 1 year | 1.27 (1.15–1.42) | 1.28 (1.16–1.43) | 1.24 (1.14–1.35) | 0.039 | 1.99 (1.78–2.30) | 1.98 (1.78–2.25) | 2.03 (1.83–2.27) | −0.475 | 418 | 285 | 5.54 | 0.22 | 260 |
| Δ, % | −17 | −18 | −17 | | −7 | −7 | −2 | | −46 | −52 | −3 | 99 | −32 |
| #005 | | | | | | | | | | | | | |
| Baseline | 1.64 (1.46–1.80) | 1.59 (1.40–1.76) | 1.65 (1.45–1.79) | −0.063 | 2.25 (2.05–2.58) | 2.29 (2.06–2.76) | 2.21 (2.04–2.39) | 0.077 | 1,018 | 656 | 12.91 | 0.09 | 698 |
| 1 year | 1.57 (1.44–1.72) | 1.52 (1.41–1.64) | 1.54 (1.41–1.70) | −0.029 | 2.24 (2.04–2.52) | 2.16 (1.96–2.41) | 2.24 (2.08–2.42) | −0.082 | 484 | 320 | NA | 0.18 | 725 |
| Δ, % | −4 | −5 | −7 | | −1 | −6 | +1 | | −49 | −51 | NA | 108 | 4 |
| #006 | | | | | | | | | | | | | |
| Baseline | 1.49 (1.38–1.64) | 1.49 (1.38–1.62) | 1.51 (1.42–1.60) | −0.021 | 1.94 (1.80–2.20) | 1.92 (1.76–2.14) | 1.90 (1.79–2.02) | 0.023 | 528 | 375 | 9.52 | 0.18 | 525 |
| 1 year | 1.57 (1.45–1.73) | 1.59 (1.46–1.76) | 1.55 (1.46–1.68) | 0.035 | 2.14 (1.94–2.43) | 2.22 (2.02–2.53) | 2.09 (1.96–2.24) | 0.125 | 723 | 482 | 5.36 | 0.14 | 450 |
| Δ, % | 5 | 7 | 3 | | 10 | 16 | 10 | | 37 | 28 | −44 | −19 | −14 |
| #007 | | | | | | | | | | | | | |
| Baseline | 1.57 (1.44–1.72) | 1.57 (1.43–1.71) | 1.52 (1.43–1.63) | 0.043 | 2.47 (2.25–2.93) | 2.60 (2.35–3.07) | 2.33 (2.18–2.50) | 0.266 | 1,423 | 1,049 | 6.62 | 0.06 | 458 |
| 1 year | 1.46 (1.34–1.60) | 1.47 (1.33–1.60) | 1.42 (1.32–1.52) | 0.046 | 2.40 (2.11–2.82) | 2.49 (2.23–2.85) | 2.25 (2.00–2.48) | 0.230 | 1,140 | 847 | 7.11 | 0.08 | 438 |
| Δ, % | −7 | −6 | −7 | | −3 | −4 | −3 | | −20 | −19 | 8 | 26 | −4 |

D and ADC parameters are reported as median (IQR). D, diffusion coefficient; ADC, apparent diffusion coefficient; RBF, renal blood flow; RPF, renal plasma flow; FF, filtration fraction; RVR, renal vascular resistance; TKV, total kidney volume; ΔD, difference between cortical and medullary D values; ΔADC, difference between cortical and medullary ADC values.

Nephron
DOI: 10.1159/000534893

**Table 3.** Clinical and laboratory findings at baseline and 1-year follow-up in the 7 patients with primary MPGN included in the study

| | #001 | #002 | #003 | #004* | #005** | #006 | #007 |
|---|---|---|---|---|---|---|---|
| C3, mg/dL | | | | | | | |
| Baseline | 19 | 6 | 15 | 22 | 14 | 24 | 11 |
| 1 year | 9 | 51 | 37 | 23 | 28 | 37 | 17 |
| Δ, % | −53 | 750 | 147 | 5 | 100 | 54 | 55 |
| uPCR, mg/g, spot | | | | | | | |
| Baseline | 4,856 | 2,355 | 2,020 | 5,715 | 3,273 | 6,211 | 573 |
| 1 year | 8,800 | 1,366 | 113 | 6,417 | NA | 10,622 | 1,118 |
| Δ, % | 81 | −42 | −94 | 12 | NA | 71 | 95 |
| uACR, mg/g, spot | | | | | | | |
| Baseline | 3,568 | 1,965 | 1,814 | 4,894 | 2,752 | 5,248 | 525 |
| 1 year | 6,875 | 1,242 | 37.4 | 5,410 | 3,366 | 8,133 | 958 |
| Δ, % | 93 | −37 | −98 | 11 | 22 | 55 | 82 |
| Urine protein, g/24 h | | | | | | | |
| Baseline | 7.3 | 1.9 | 8.9 | 6.8 | 6.4 | 7.8 | 1.9 |
| 1 year | 9.5 | 2.9 | 0.2 | 6 | 10.55 | 12.6 | 1.1 |
| Δ, % | 30 | 53 | −98 | −12 | 65 | 62 | −42 |
| Serum total protein, g/dL | | | | | | | |
| Baseline | 3.8 | 3.9 | 5.6 | 4.2 | 3.9 | 4.9 | 5.9 |
| 1 year | 4.6 | 4.8 | 6.5 | 5 | 3.6 | 4.5 | 5.7 |
| Δ, % | 21 | 23 | 16 | 19 | −8 | −8 | −3 |
| Serum albumin, g/dL | | | | | | | |
| Baseline | 2.2 | 2.4 | 3.7 | 2.2 | 2.2 | 2.7 | 3.6 |
| 1 year | 2.8 | 3.1 | 4.1 | 3 | 1.9 | 2.9 | 3.6 |
| Δ, % | 27 | 29 | 11 | 36 | −14 | 7 | 0 |
| Serum creatinine, mg/dL | | | | | | | |
| Baseline | 2.3 | 0.4 | 1.3 | 1.2 | 0.7 | 1.4 | 1.2 |
| 1 year | 5.8 | 0.4 | 1.1 | 2.7 | 1.4 | 1.7 | 1.3 |
| Δ, % | 152 | 0 | −15 | 125 | 100 | 21 | 8 |
| eGFR, mL/min/1.73 $m^2$ | | | | | | | |
| Baseline | 35.2 | 143.7 | 78.8 | 64.6 | 132.5 | 50.7 | 80.8 |
| 1 year | 11.7 | 148 | 89.8 | 24.7 | 67.6 | 41 | 72.7 |
| Δ, % | −67 | 3 | 14 | −62 | −49 | −19 | −10 |
| mGFR, mL/min/1.73 $m^2$ | | | | | | | |
| Baseline | 36.04 | 87.56 | 46.82 | 33.78 | 84.73 | 35.71 | 69.38 |
| 1 year | 13.37 | 119.72 | 74.56 | 15.77 | NA | 25.84 | 60.24 |
| Δ, % | −63 | 37 | 59 | −53 | NA | −28 | −13 |

C3, complement component 3; uPCR, urinary protein to creatinine ratio; uACR, urinary albumin to creatinine ratio; eGFR, GFR estimated by the CKD-EPI formula; mGFR, GFR measured by iohexol clearance; NA, not available. *1 year data refer to week 65 instead of week 52. **1 year data refer to 9 months (instead of 12 months) follow-up.

uACR was negatively associated with RBF, RPF, and FF (rho = −0.86, $p < 0.001$, rho = −0.84, $p < 0.001$, and rho = −0.6, $p = 0.043$, respectively), while positively correlated with RVR (rho = 0.88, $p < 0.001$). No correlation was found between uACR and diffusivity at individual time points (Fig. 3a).

Considering the disease course in individual patients, a decrease in uACR was associated with an increase in kidney and cortex diffusivity (rho = −0.5, $p = 0.27$ and rho = −0.64, $p = 0.14$, respectively) (Fig. 3b). mGFR was positively associated with diffusivity in the kidney, cortex, and medulla (rho = 0.59, $p = 0.034$; rho = 0.52, $p = 0.068$; rho = 0.57, $p = 0.041$), with RBF, RPF, and FF (rho = 0.87, $p < 0.001$; rho = 0.68, $p = 0.019$; rho = 0.85, $p < 0.001$), while negatively correlated with RVR (rho = −0.89, $p < 0.001$) (Fig. 4a). An increase in mGFR after 1-year follow-up was associated with an increase in diffusivity in the kidney, cortex, and medulla (rho = 0.77, $p = 0.1$; rho = 0.83,

**Table 4.** Histologic findings at baseline kidney biopsy in the 7 patients with primary MPGN included in the study

| | #001 | #002 | #003 | #004 | #005 | #006 | #007 |
|---|---|---|---|---|---|---|---|
| Qualitative evaluation | | | | | | | |
| Predominant pattern | MPGN | MPGN | MPGN | MPGN | MPGN | MPGN | MPGN |
| Glomeruli, *n* | 11 | 14 | 19 | 15 | 8 | 19 | 12 |
| Global sclerosis, % | 27 | 14 | 5 | 30 | 25 | 21 | 8 |
| Segmental sclerosis, % | 60 | 35 | 10 | 40 | 25 | 60 | 25 |
| Mesangial proliferation (0–3) | 2 | 2 | 3 | 2 | 2 | 2 | 2 |
| Membranoproliferative features (0–3) | 3 | 3 | 3 | 3 | 2 | 3 | 2 |
| Leukocyte infiltration (0–3) | 3 | 2 | 3 | 3 | 2 | 2 | 3 |
| Crescents, % | 0 | 0 | 20 | 0 | 0 | 0 | 0 |
| Quantitative evaluation | | | | | | | |
| Fibrosis, % | 3.5 | 4.0 | 6.4 | 4.1 | 5.3 | 6.3 | 4.1 |
| Peritubular interstitial volume, % | 36.6 | 18.6 | 25.1 | 39.7 | 40.3 | 38.1 | 22.5 |

MPGN, membranoproliferative glomerulonephritis.

$p = 0.058$; rho = 0.77, $p = 0.1$), RBF, RPF, and FF (rho = 0.7, $p = 0.23$ in all cases), and total kidney volume (rho = 0.54, $p = 0.3$), and with a decrease in RVR (rho = −0.7, $p = 0.23$) (Fig. 4b).

Table 5 shows the comparison between MRI and clinical parameters' changes in the individual patients included in the study. Possible correlations between baseline MRI biomarkers and change in mGFR and uACR have been investigated. Despite the limited sample size, there seems to be a positive correlation between baseline RBF/FF and 1-year mGFR change (rho = 0.54 and 0.6, respectively), and a negative correlation between baseline RVR and 1-year mGFR change (rho = −0.6) (online suppl. Fig. 1).

## Discussion

This study provides evidence in support of kidney functional MRI potential to monitor disease course in primary MPGN. Functional MRI markers, allowing to noninvasively assess kidney structural and functional changes in vivo, correlated with clinical characteristics in patients at different stages of the disease. Indeed, MRI-based perfusion parameters correlated with kidney function and albuminuria at individual time points, while diffusivity parameters proved useful to assess changes in clinical parameters.

At difference with previous studies, in our patients we separately quantified interstitial fibrosis and peritubular interstitial volume in kidney biopsies. Of relevance, MRI-based perfusion parameters were negatively associated with peritubular interstitial volume, while RVR was positively associated with it. Conversely, no significant correlation was found between any MRI parameter and interstitial fibrosis, at difference with other previous evidence in CKD and kidney allograft patients [15, 16, 20, 21], likely due to the limited sample size inherent with rare disease investigations. Our finding on peritubular interstitial volume is however in line with a recent study [17] and can be explained by the fact that in case of pathological involvement, the interstitium not only increases in volume due to accumulation of fibrotic extracellular matrix but also due to proliferation of fibroblasts and renin-producing perivascular cells [18], further expanding the cortical area occupied by the interstitium. Cortical peritubular interstitial volume, rather than interstitial fibrosis – an unlikely reversible chronic kidney damage – may decrease in case of favorable disease course and could represent a possible therapeutic target. In case of interstitial damage, peritubular capillaries are not well-organized anymore, causing reduced renal perfusion and increased microvasculature resistance explaining the observed correlations.

Serum C3 positively correlated with diffusivity, RBF and FF, and negatively with RVR. Since reduced C3 in serum indicates massive complement activation leading to increased deposits of activation products and renal damage, the observed correlations highlight an indirect association between MRI biomarkers and C3 deposits in the kidney.

In a large cohort of primary MPGN patients, using a composite outcome, authors found that risk of progression to kidney failure associated with eGFR and proteinuria at the time of biopsy, cellular/fibrocellular crescents, segmental sclerosis and interstitial fibrosis/

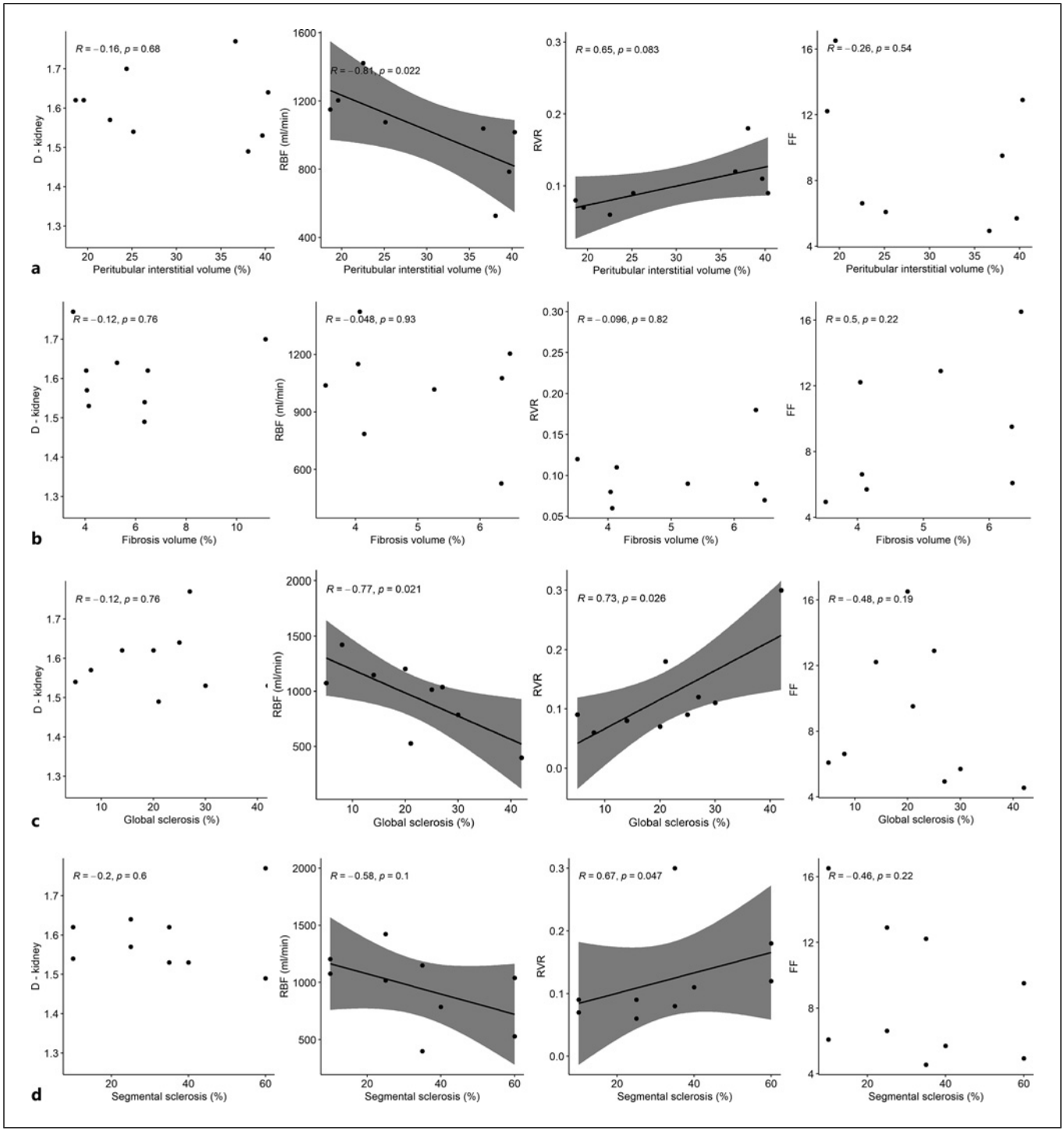


**Fig. 1.** Correlation between MRI and histologic findings at all available time points in the 7 patients with primary MPGN included in the study. **a** Correlation between MRI parameters and peritubular interstitial volume. **b** Correlation between MRI parameters and interstitial fibrosis. **c** Correlation between MRI parameters and global glomerular sclerosis. **d** Correlation between MRI parameters and segmental glomerular sclerosis. D, diffusion coefficient; RBF, renal blood flow; FF, filtration fraction; RVR, renal vascular resistance.

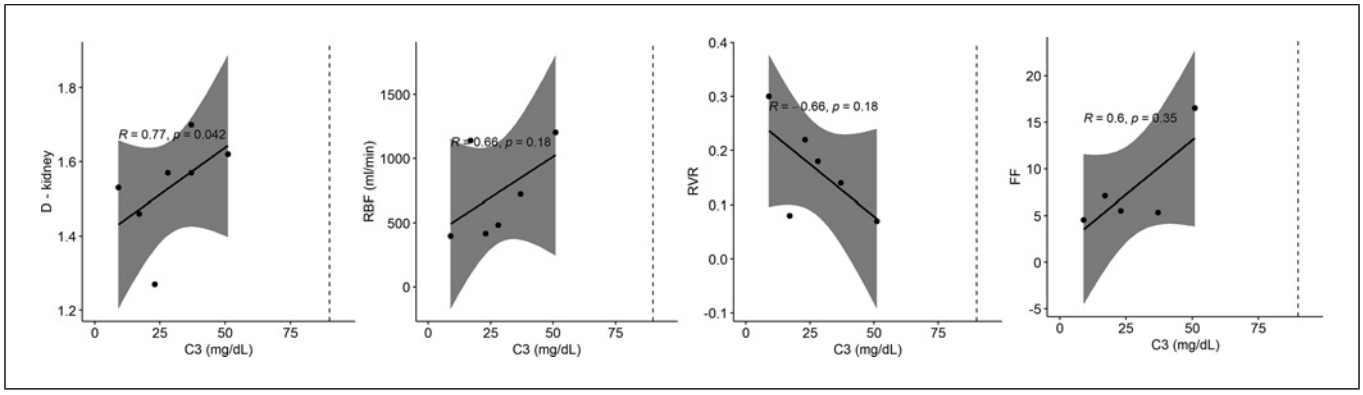


**Fig. 2.** Correlation between C3 and MRI parameters at 1-year follow-up in the 7 patients with primary MPGN included in the study. Dashed lines denote C3 lower limit of normality (90 mg/dL). D, diffusion coefficient; RBF, renal blood flow; FF, filtration fraction; RVR, renal vascular resistance.

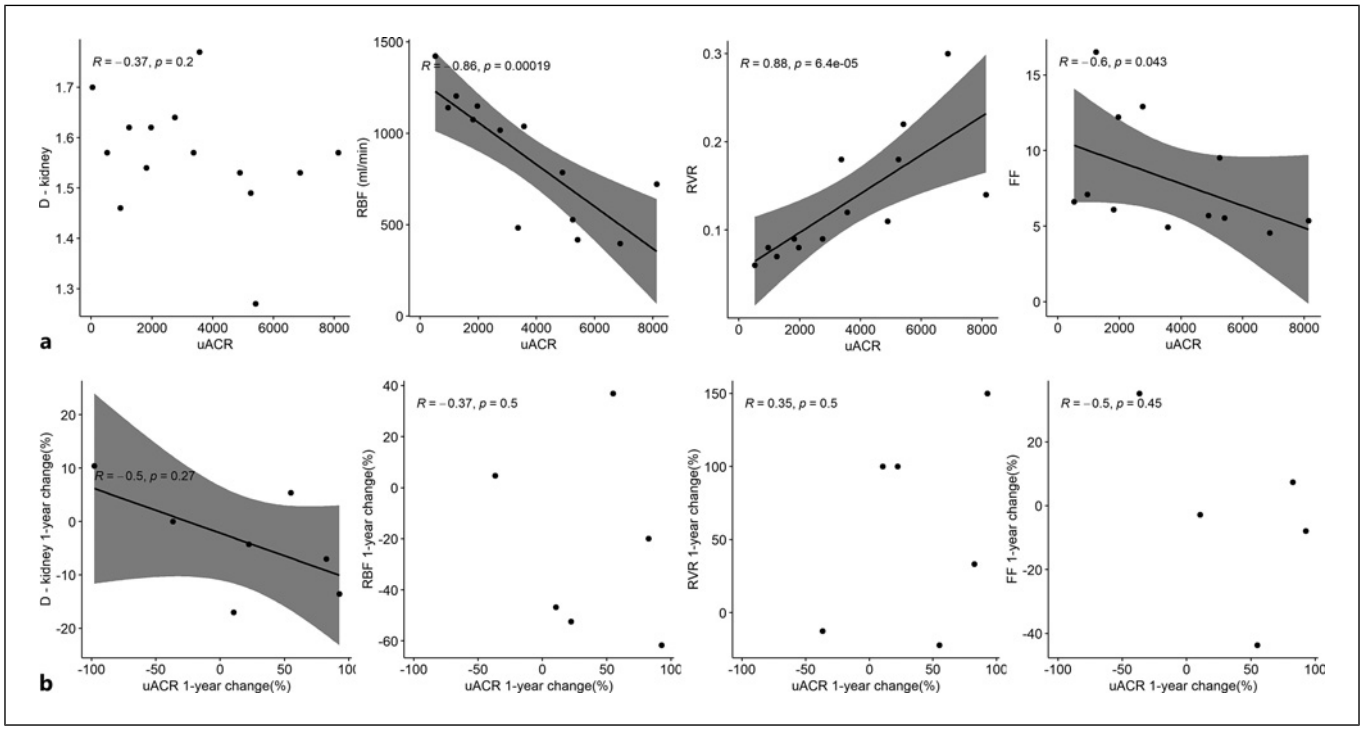


**Fig. 3.** Correlation between uACR and MRI parameters in the 7 patients with primary MPGN included in the study. **a** Correlation at all available time points (baseline and 1-year follow-up). **b** Correlation between changes after 1-year follow-up. uACR normality range = [0.0–19.9]. D, diffusion coefficient; RBF, renal blood flow; FF, filtration fraction; RVR, renal vascular resistance.

tubular atrophy scores [19]. Similarly, in our study, mGFR and uACR at baseline associated with functional MRI markers, which precisely reflect renal damage and parenchymal changes. Among the histologic parameters, we found that global and segmental glomerular sclerosis were negatively associated with RBF and RPF and positively with RVR, indicating a possible detrimental effect of the two histologic features on renal function.

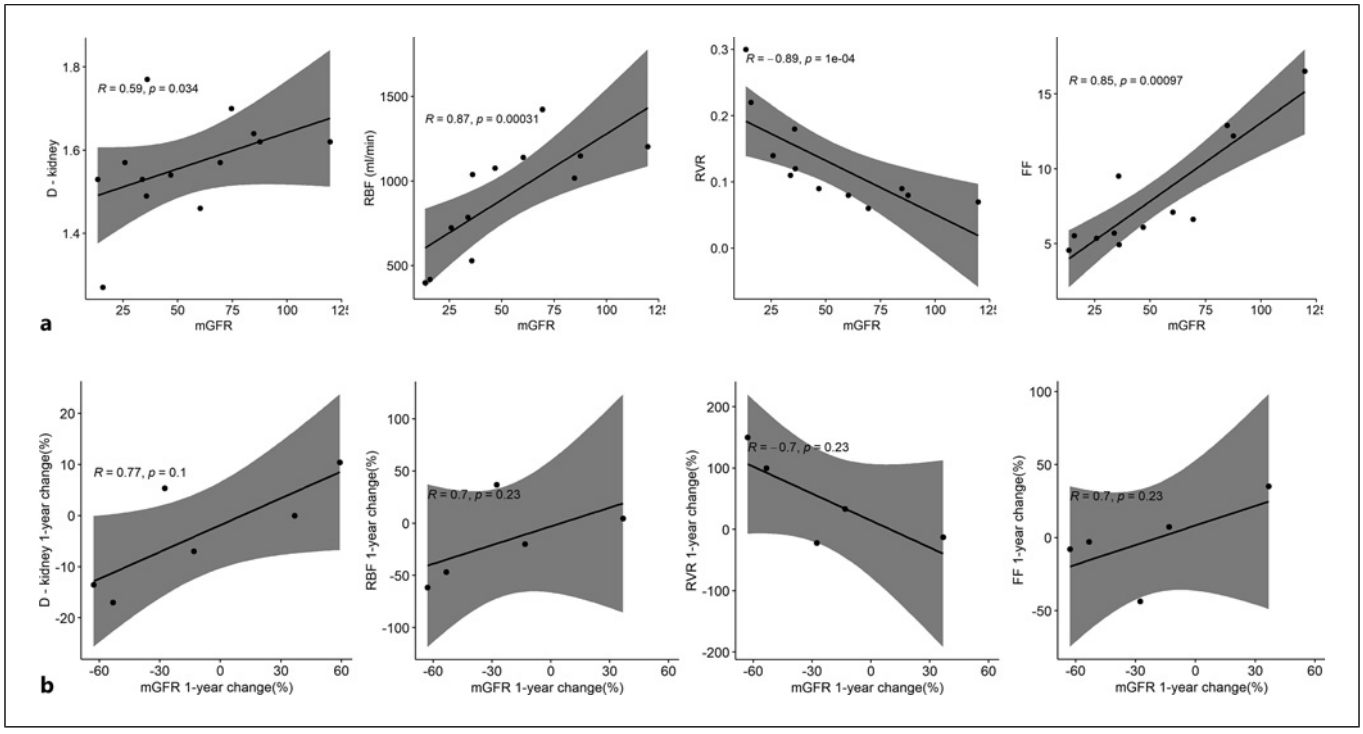


**Fig. 4.** Correlation between measured GFR (mGFR) and MRI parameters in the 7 patients with primary MPGN included in the study. **a** Correlation at all available time points (baseline and 1-year follow-up). **b** Correlation between changes after 1-year follow-up. mGFR normality range >60. D, diffusion coefficient; RBF, renal blood flow; FF, filtration fraction; RVR, renal vascular resistance.

**Table 5.** Comparison between changes in key MRI and clinical parameters in the 7 patients with primary MPGN included in the study

| | MRI parameters' change | | | | Clinical parameters' change | |
|---|---|---|---|---|---|---|
| | Δ $D_{kidney}$ | Δ RBF | Δ RPF | Δ RVR | Baseline mGFR (ml/min/1.73m²) | Δ mGFR (ml/min/1.73m²) |
| **#001** | -14% | -62% | -60% | +158% | 36.04 | -22.67 |
| **#002** | 0% | +5% | +1% | -14% | 87.56 | +32.16 |
| **#003** | +11% | NA | NA | NA | 46.82 | +27.74 |
| **#004** | -17% | -46% | -52% | +99% | 33.78 | -18.01 |
| **#005** | -4% | -49% | -51% | +108% | 84.73 | NA |
| **#006** | +5% | +37% | +28% | -19% | 35.71 | -9.87 |
| **#007** | -7% | -20% | -19% | +26% | 69.38 | -9.14 |

A traffic-light color coding was used, with green, orange, and red indicating positive, not relevant/partial, and negative changes. Color coding was based on the following thresholds: Δ $D_{kidney}$: green ≥0%, yellow [−10 to −1]%, red: <−10%; Δ RBF, Δ RPF and Δ RVR: green ≥0%, yellow [−20 to −1]%, red: <−20%; Δ GFR: green ≥0 mL/min/1.73 $m^2$, yellow [−10 to −1] mL/min/1.73 $m^2$, red: <−10 mL/min/1.73 $m^2$. D, diffusion coefficient; RBF, renal blood flow; RPF, renal plasma flow; RVR, renal vascular resistance; mGFR, GFR measured by iohexol clearance; NA, not available.

To the best of our knowledge, this is the first study investigating kidney MRI potential in patients with primary MPGN rare disease. Despite several cross-sectional studies showing the association between DWI or PC-MRI parameters and kidney function in kidney diseases [9, 10], longitudinal evidence of their clinical validity in monitoring disease progression is still limited. Berchtold and colleagues showed DWI potential in detecting an increase in interstitial

fibrosis, even earlier than renal function decline [20], and in predicting kidney function decline in CKD and kidney allograft [22]. In the context of a recent multicenter clinical study, Srivastava and colleagues found an association between baseline DWI parameters and eGFR change over time that was not independent of albuminuria [23]. Khatir and colleagues successfully used PC-MRI to assess changes in RVR in CKD patients in response to vasodilating and non-vasodilating therapy [24]. Torres and colleagues showed that PC-MRI-based RBF reduction precedes GFR decline and predicts disease progression in polycystic kidney disease [25]. Last, current findings are in line with a recent study showing a good correlation between multiparametric MRI and available measures of renal function and pathology in healthy volunteers and CKD patients [26]. As in our case, a positive correlation between RBF and GFR and a negative correlation between RBF and uPCR were observed.

Limitations of this study include the small number of patients. However, since primary MPGN is a rare disease, the size of the patient population under study is relevant. Moreover, the significant correlations obtained in such a small sample further highlight the promise of the study findings. Current evaluations took account of parameters at individual time points. While the correlation between changes over time in MRI biomarkers and clinical parameters was assessed, it was not possible to evaluate changes in histological features since only 2/7 patients undergo follow-up biopsy. Future studies are needed to investigate this aspect. In addition, it should be pointed out that, while the associations of MRI parameters with clinical features are encouraging, its clinical utility in monitoring efficacy of intervention still needs to be proved. Our preliminary findings suggest a stronger correlation between change in MRI parameters and clinical outcome in patients with mildly decreased renal function. Disease progression in advanced stages may be indeed independent of treatment targeted at complement inhibition and more appropriately monitored through easily available laboratory tests.

Beyond DWI and PC-MRI, there are several other NCE-MRI techniques noninvasively providing complementary information on renal tissue perfusion, oxygenation, and microstructure [7, 27]. A few recent studies have shown multiparametric MRI to be feasible in patients with kidney disease in a single scan session of less than an hour [23, 26]. Moreover, recent standardization efforts have provided consensus recommendations on kidney MRI acquisition and analysis [28–32], thus improving comparability of different study results. Multiparametric kidney MRI may further improve the understanding of kidney pathophysiology and accurate monitoring of disease progression.

In conclusion, the strong significant correlation found between MRI-based parameters and histologic and clinical findings, despite the rather limited number of patients, highlights MRI potential to monitor disease progression in rare kidney diseases. Whilst renal biopsy remains crucial for diagnosis, functional MRI could integrate repeated biopsy for monitoring disease progression. Future larger studies are needed to confirm current findings and demonstrate benefits and cost effectiveness of multiparametric MRI in kidney disease management.


## Acknowledgments

The authors wish to thank all patients participating in the study.


## Statement of Ethics

This study was conducted ethically in accordance with the World Medical Association Declaration of Helsinki. The study was reviewed and approved by the Local Ethics Committee (Comitato Etico della Provincia di Bergamo), approval number 179-18. Written informed consent was obtained from all adults or parents for minor patients.

## Conflict of Interest Statement

The authors have no conflicts of interest to declare.


## Funding Sources

This study was supported in part by Alexion Pharmaceuticals, Boston, MA, USA.


## Author Contributions

Giulia Villa, Erica Daina, and Anna Caroli substantially contributed to the conception and design of the work and drafted the manuscript. Giulia Villa, Erica Daina, Paolo Brambilla, Sara Gamba, Valentina Fanny Leone, Camillo Carrara, Paola Rizzo, Marina Noris, Giuseppe Remuzzi, Andrea Remuzzi, and Anna Caroli substantially contributed to the acquisition, analysis, or interpretation of data for the work. Paolo Brambilla, Sara Gamba, Valentina Fanny Leone, Camillo Carrara, Paola Rizzo, Marina Noris, Giuseppe Remuzzi, and Andrea Remuzzi critically reviewed the paper draft for important intellectual content. Giulia Villa, Erica Daina, Paolo Brambilla, Sara Gamba, Valentina Fanny Leone, Camillo Carrara, Paola Rizzo, Marina Noris, Giuseppe Remuzzi, Andrea Remuzzi, and Anna Caroli approved the final

version of the manuscript and agree to be accountable for all aspects of the work in ensuring that questions related to the accuracy or integrity of any part of the work are appropriately investigated and resolved.

## Data Availability Statement

The data that support the findings of this study are available from the corresponding author, upon reasonable request.

## References


1 Cook HT, Pickering MC. Histopathology of MPGN and C3 glomerulopathies. Nat Rev Nephrol. 2015;11(1):14–22.
2 Sethi S, Fervenza FC. Membranoproliferative glomerulonephritis--a new look at an old entity. N Engl J Med. 2012;366(12):1119–31.
3 Sethi S, Fervenza FC. Membranoproliferative glomerulonephritis: pathogenetic heterogeneity and proposal for a new classification. Semin Nephrol. 2011;31(4):341–8.
4 Pickering MC, D'Agati VD, Nester CM, Smith RJ, Haas M, Appel GB, et al. C3 glomerulopathy: consensus report. Kidney Int. 2013;84(6):1079–89.
5 Iatropoulos P, Daina E, Curreri M, Piras R, Valoti E, Mele C, et al. Cluster analysis identifies distinct pathogenetic patterns in C3 glomerulopathies/immune complex-mediated membranoproliferative GN. J Am Soc Nephrol. 2018;29(1):283–94.
6 Servais A, Noël LH, Roumenina LT, Le Quintrec M, Ngo S, Dragon-Durey MA, et al. Acquired and genetic complement abnormalities play a critical role in dense deposit disease and other C3 glomerulopathies. Kidney Int. 2012;82(4):454–64.
7 Caroli A, Pruijm M, Burnier M, Selby NM. Functional magnetic resonance imaging of the kidneys: where do we stand? The perspective of the European COST Action PARENCHIMA. Nephrol Dial Transplant. 2018;33(suppl l_2):ii1–ii3.
8 Selby NM, Blankestijn PJ, Boor P, Combe C, Eckardt KU, Eikefjord E, et al. Magnetic resonance imaging biomarkers for chronic kidney disease: a position paper from the European Cooperation in Science and Technology Action PARENCHIMA. Nephrol Dial Transplant. 2018;33(suppl l_2):ii4–ii14.
9 Caroli A, Schneider M, Friedli I, Ljimani A, De Seigneux S, Boor P, et al. Diffusion-weighted magnetic resonance imaging to assess diffuse renal pathology: a systematic review and statement paper. Nephrol Dial Transplant. 2018;33(Suppl l_2):ii29–40.
10 Villa G, Ringgaard S, Hermann I, Noble R, Brambilla P, Khatir DS, et al. Phase-contrast magnetic resonance imaging to assess renal perfusion: a systematic review and statement paper. Magn Reson Mater Phy. 2020;33(1):3–21.
11 Rasband. ImageJ. US National Institutes of Health. Bethesda, Maryland, USA. Available from: http://imagej.nih.gov/ij.
12 Bomback AS, Santoriello D, Avasare RS, Regunathan-Shenk R, Canetta PA, Ahn W, et al. C3 glomerulonephritis and dense deposit disease share a similar disease course in a large United States cohort of patients with C3 glomerulopathy. Kidney Int. 2018;93(4):977–85.
13 Gaspari F, Perico N, Ruggenenti P, Mosconi L, Amuchastegui CS, Guerini E, et al. Plasma clearance of nonradioactive iohexol as a measure of glomerular filtration rate. J Am Soc Nephrol. 1995;6(2):257–63.
14 Levey AS, Stevens LA, Schmid CH, Zhang YL, Castro AF 3rd, Feldman HI, et al. A new equation to estimate glomerular filtration rate. Ann Intern Med. 2009;150(9):604–12.
15 Hua C, Qiu L, Zhou L, Zhuang Y, Cai T, Xu B, et al. Value of multiparametric magnetic resonance imaging for evaluating chronic kidney disease and renal fibrosis. Eur Radiol. 2023;33(8):5211–21.
16 Mao W, Ding X, Ding Y, Cao B, Fu C, Kuehn B, et al. Evaluation of interstitial fibrosis in chronic kidney disease by multiparametric functional MRI and histopathologic analysis. Eur Radiol. 2023;33(6):4138–47.
17 Caroli A, Remuzzi A, Ruggiero B, Carrara C, Rizzo P, Brambilla P, et al. Functional magnetic resonance imaging versus kidney biopsy to assess response to therapy in nephrotic syndrome: a case report. Kidney Med. 2020;2(6):804–9.
18 Zeisberg M, Kalluri R. Physiology of the renal interstitium. Clin J Am Soc Nephrol. 2015;10(10):1831–40.
19 Lomax-Browne HJ, Medjeral-Thomas NR, Barbour SJ, Gisby J, Han H, Bomback AS, et al. Association of histologic parameters with outcome in C3 glomerulopathy and idiopathic immunoglobulin-associated membranoproliferative glomerulonephritis. Clin J Am Soc Nephrol. 2022;17(7):994–1007.
20 Berchtold L, Friedli I, Crowe LA, Martinez C, Moll S, Hadaya K, et al. Validation of the corticomedullary difference in magnetic resonance imaging-derived apparent diffusion coefficient for kidney fibrosis detection: a cross-sectional study. Nephrol Dial Transplant. 2020;35(6):937–45.
21 Zhu J, Chen A, Gao J, Zou M, Du J, Wu PY, et al. Diffusion-weighted, intravoxel incoherent motion, and diffusion kurtosis tensor MR imaging in chronic kidney diseases: correlations with histology. Magn Reson Imaging. 2023;S0730-725X(23):00118–2.
22 Berchtold L, Crowe LA, Combescure C, Kassaï M, Aslam I, Legouis D, et al. Diffusion-Magnetic Resonance Imaging predicts decline of kidney function in chronic kidney disease and in patients with a kidney allograft. Kidney Int. 2022;101(4):804–13. S0085253821012151.
23 Srivastava A, Cai X, Lee J, Li W, Larive B, Kendrick C, et al. Kidney functional magnetic resonance imaging and change in eGFR in individuals with CKD. Clin J Am Soc Nephrol. 2020;15(6):776–83.
24 Khatir DS, Pedersen M, Ivarsen P, Christensen KL, Jespersen B, Buus NH. Effects of additional vasodilatory or nonvasodilatory treatment on renal function, vascular resistance and oxygenation in chronic kidney disease: a randomized clinical trial. J Hypertens. 2019;37(1):116–24.
25 Torres VE, King BF, Chapman AB, Brummer ME, Bae KT, Glockner JF, et al. Magnetic resonance measurements of renal blood flow and disease progression in autosomal dominant polycystic kidney disease. Clin J Am Soc Nephrol. 2007;2(1):112–20.
26 Buchanan CE, Mahmoud H, Cox EF, McCulloch T, Prestwich BL, Taal MW, et al. Quantitative assessment of renal structural and functional changes in chronic kidney disease using multi-parametric magnetic resonance imaging. Nephrol Dial Transplant. 2020;35(6):955–64.
27 Pruijm M. Can COMBINED magnetic resonance imaging measure the progression of kidney disease? Clin J Am Soc Nephrol. 2020;15(6):747–9.
28 Bane O, Mendichovszky IA, Milani B, Dekkers IA, Deux JF, Eckerbom P, et al. Consensus-based technical recommendations for clinical translation of renal BOLD MRI. Magn Reson Mater Phy. 2020;33(1):199–215.
29 de Boer A, Villa G, Bane O, Bock M, Cox EF, Dekkers IA, et al. Consensus-based technical recommendations for clinical translation of renal phase contrast MRI. J Magn Reson Imaging. 2022;55(2):323–35.
30 Dekkers IA, de Boer A, Sharma K, Cox EF, Lamb HJ, Buckley DL, et al. Consensus-based technical recommendations for clinical translation of renal T1 and T2 mapping MRI. Magn Reson Mater Phy. 2020;33(1):163–76.
31 Ljimani A, Caroli A, Laustsen C, Francis S, Mendichovszky IA, Bane O, et al. Consensus-based technical recommendations for clinical translation of renal diffusion-weighted MRI. Magn Reson Mater Phy. 2020;33(1):177–95.
32 Nery F, Buchanan CE, Harteveld AA, Odudu A, Bane O, Cox EF, et al. Consensus-based technical recommendations for clinical translation of renal ASL MRI. Magn Reson Mater Phy. 2020;33(1):141–61.